A NOVEL OPTICAL/DIGITAL PROCESSING SYSTEM FOR PATTERN RECOGNITION

Bradley G. Boone and Oodaye B. Shukla

Johns Hopkins University Applied Physics Laboratory
Electro-Optical Systems Group
Johns Hopkins Road, Laurel, MD 20723-6099

ABSTRACT

This paper describes two processing algorithms that can be implemented optically: the Radon transform and angular correlation. These two algorithms can be combined in one optical processor to extract all the basic geometric and amplitude features from objects embedded in video imagery. We show that the internal amplitude structure of objects is recovered by the Radon transform, which is a well-known result, but, in addition, we show simulation results that calculate angular correlation, a simple but unique algorithm that extracts object boundaries from suitably thresholded images from which length, width, area, aspect ratio, and orientation can be derived. In addition to circumventing scale and rotation distortions, these simulations indicate that the features derived from the angular correlation algorithm are relatively insensitive to tracking shifts and image noise. Some optical architecture concepts, including one based on micro-optical lenslet arrays, have been developed to implement these algorithms. Simulation test and evaluation using simple synthetic object data will be described, including results of a study that uses object boundaries (derivable from angular correlation) to classify simple objects using a neural network.

1. INTRODUCTION

Optics and pattern recognition are key areas for systems development for both DoD and civilian applications, including tactical missile guidance, strategic surveillance, optical parts inspection, medical imaging and non-destructive evaluation. Both passive imaging sensors (infrared (IR) and visible) and active microwave imaging sensors have been employed in many systems to date, but pattern recognition solutions in conjunction with these sensors are highly application dependent and have required extensive training. These factors have precluded extensive development.

The objective of this paper is to describe the concept of an optical processor for object measurement that can be interfaced to a variety of sensors, including imaging IR, optical machine vision systems and synthetic aperture radar (SAR), thus making it very versatile. The optical processor will be used in conjunction with a neural network algorithm to classify objects. Another goal is to provide a preliminary report on the effectiveness of the measurement and classification algorithms that we plan to implement with optics and digital electronics, respectively.

One of the key concerns in the design of optical feature extractors and image matchers for target recognition is that performance be invariant with respect to position, scale and rotation distortions. In many cases traditional approaches have involved complicated mathematical transformations to achieve distortion invariance[1-2]. Our approach[3-5] offers a compact distortion-insensitive method of optical correlation using primitive image operations such as image replication, multiplication, integration, and detection, and is useful in viewing objects in plan-view. One of the key aspects of this approach is that we use optical correlation to measure objects rather than match them. We leave the matching up to a neural network.

Our optical processor[5] concept implements the optical Radon (or Hough) transform and the APL developed optical angular correlation technique, followed by appropriate numerical processing, and a neural net classifier. The angular correlator is a unique development that enables object symmetry, orientation, primitive dimensions and boundary to be estimated. Along with the well-developed Hough transform, which provides information on the internal structure of objects, these features collectively describe most simple closed-boundary objects in an elegant and compact way, thus affording generic object measurement and the prospect of effective object classification. The only major requirements for this processor are that the input imaging sensor employ

detection with adaptive thresholding and centroid tracking, both of which are common (or easily implemented) attributes of most imaging sensors.

The key components of this overall concept are laid out in Figure 1. Basically, the overall system consists of four stages: an optical interface to an appropriate sensor display or entrance optics, optical processor for angular correlation and (optional) Hough transform, digital processor for calculating various features of the object data, and finally, a digital or analog neural network. Either of two techniques have been considered for rotating input imagery: video feedback (time-multiplexing) or multiple aperture optics (space-multiplexing). (However, image rotation is not critical to implementing the angular correlation algorithm.) Early efforts[6-7] using video feedback explored the Hough transform and angular correlation in a single-channel (time-multiplexed) implementation. Similar concepts in multi-aperture optical processors have been proposed for these and other applications[9-12] and offer smaller size and increased throughput.

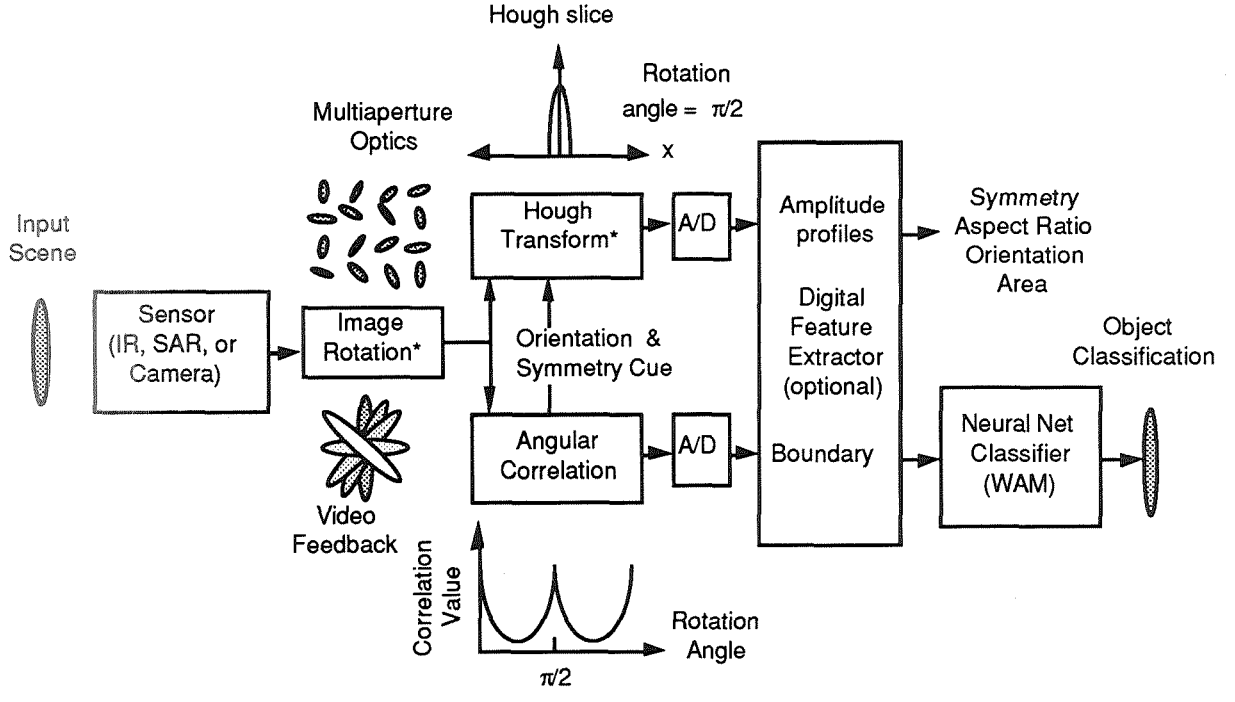

Figure 1. Block diagram of angular correlator architecture (items denoted by * are optional).

What we will concentrate on in this paper is the evaluation of a simulation of the angular correlation algorithm in conjunction with a winner-take-all associative memory (WAM) neural net. Both of these algorithms were developed at JHU/APL and are currently in the process of implementation. Some aspects of the implementation of the angular correlator will also be described.

2. ANGULAR CORRELATION

Many kinds of correlation algorithms have been implemented for pattern matching applications. Most correlation algorithms shift one image with respect to the other while calculating the area of overlap. Angular correlation simply calculates the area of overlap versus angle. The resulting set of correlation values can be used to recover the boundary of an object if the object is thresholded and binarized and the other object is a slit. Since the angular correlation algorithm uses rotation, the need for rotational invariance is obviated. Scale invariance is irrelevant to angular correlation because it measures an object. The optical implementation uses incoherent light (allowing the use of standard camera optics or video displays as image inputs) and multi-aperture optics (making it light-weight and compact using off-the-shelf components).

Primitive features of an object can also be determined by using angular correlation. Object primitives include: area, length, width, aspect ratio, symmetry, and orientation. For most simple objects periodicity of the boundary is directly related to symmetry. For a square (which has four-fold symmetry), the periodicity is $\pi/2$ ($2\pi/4$), whereas for an equilateral triangle (three-fold symmetry), the periodicity is $2\pi/3$. With the object centered, the peak values of the recovered boundary are related to the maximum extent of the object. The minimum value of the boundary curve is the minimum dimension of the object through its centroid. Taking the ratio of the maximum and minimum values of the recovered boundary yields the aspect ratio of a simple two-fold symmetric object like a rectangle or an ellipse. The minimum value of the recovered boundary curve (or "bias") is also a measure of the image "mass" concentration of the object about its centroid. For example, the boundary of a star shaped object is a set of periodic peaks with a lower bias than the boundary of a square which has more image "mass" at its center (see Figure 5).

For angular correlation, both objects have to be centered with respect to a common origin. In that case the maximum correlation value gives the cue for selection of an optimal Radon transform slice. The peak correlation values for offset slits are less than the peak correlation value of a slit with no offset as shown in Fig. 2(a). Even for large offsets the periodicity and optimum cueing angle remain unchanged. Thus a key assumption necessary for implementing this algorithm digitally or optically is that the object be centroid tracked, something often achieved in practice with imaging sensors and good tracking systems.

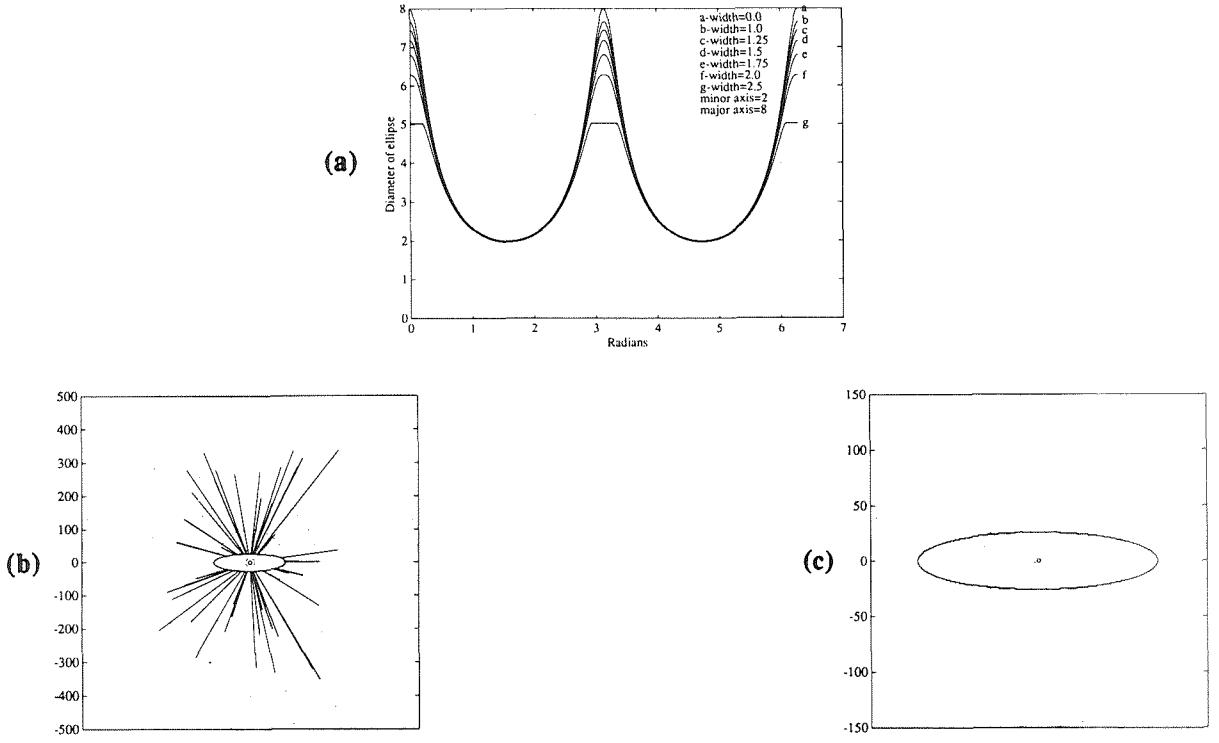

Figure 2. (a) Angular correlation of ellipse for varying offsets of correlation slit, (b) polar plot of ellipse with substantial image noise (SNR ≈ 8), and (c) cleaned-up ellipse boundary using a thresholded first-forward difference filter.

Consider the angular cross-correlation of a slit (extending over the entire image) with an ellipse in more detail. When the slit and the major axis of the ellipse are oriented horizontally, the area of overlap is approximately the width of the slit multiplied by the major axis of the ellipse. By decreasing the slit width, the intersecting area approaches the length of the major axis of the ellipse. As the slit is rotated, the area of overlap is the boundary of the object at the slit angle. Angular cross-correlation for binarized images can then be expressed mathematically as:

$$R(\theta) = \int_0^{\infty} \int_0^{\infty} \text{rect}\left[\frac{r}{r(\theta')}\right] \text{rect}\left[\frac{r}{r_{rect}(\theta' + \theta)}\right] r dr d\theta' \tag{1}$$

where $\text{rect}[r/r_{rect}(\theta' + \theta)]$ is a functional description of a rectangular slit rotated by an angle θ, and $\text{rect}[r/r(\theta')]$ is the corresponding description for the desired object.

Ideally the slit width should approach zero to recover the exact boundary of an object, but in practice we must measure a finite signal. The minimum sampling angle necessary to sample the boundary of an object and to satisfy the Nyquist sampling criterion can be calculated by examining the Fourier spectrum of the boundary function to obtain the cutoff frequency. Then the appropriate slit width can be determined from this using simple geometry. Essentially this means that complex binarized objects should be cross-correlated with a slit one pixel wide. In the digital simulation, the slit is rotated while the image remains fixed. If the image is noise-free, then the boundary recovered is exact. However if the image is extremely noisy, then the recovered boundary will have spikes on it as shown in Figure 2(b). A noisy boundary can be filtered to recover the smooth boundary by using the Nyquist bandwidth of the boundary function to set a low-pass filter cutoff (or by using a first-forward difference with a limiting threshold as was done for Fig. 2(c)).

The angular correlation algorithm is effective on simple convex shapes, such as rectangles, triangles, ellipses, and circles, and some concave shapes such as stars and gears. Objects that do not have simple closed boundaries are those with re-entrant boundaries and multiple boundaries, as shown in Figure 3. For objects with such boundaries, the estimated boundary recovered by angular correlation will not necessarily enable it to be discriminated from other (simpler) boundaries because only the total area of overlap is recovered. In other words, the area of overlap between the slit and object is a single value that does not contain any information about boundaries within the slit.

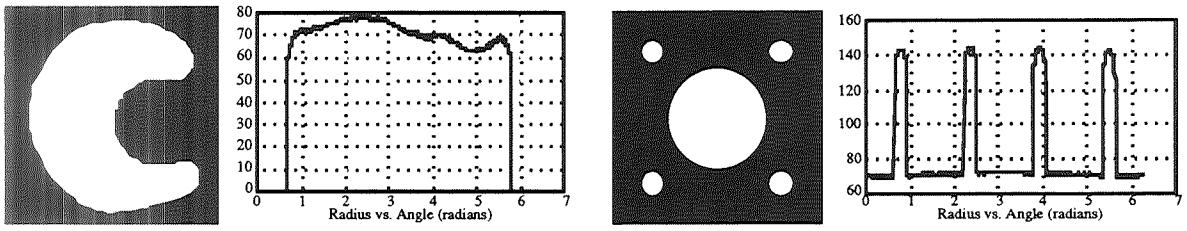

Figure 3. **Objects and boundary functions of shapes with (a) re-entrant boundaries and (b) multiple boundaries.**

3. HOUGH TRANSFORM

The Hough (or Radon) transform is a well known mathematical transform used in image processing to reconstruct objects. The Radon transform is a collection of 1-D projections. For each angle θ, an object's amplitude projection is obtained by integration perpendicular to the p-axis (which is the x-axis rotated by θ). The complete Radon transform is given by:

$$F_R(p,\theta) = \int_{-\infty}^{\infty} \int_{-\infty}^{\infty} f(\mathbf{r})\, \delta(p - \mathbf{r}\cdot\mathbf{n})\, d^2\mathbf{r} \tag{2}$$

where the 2-D object is defined by the function $f(\mathbf{r})$ and $\mathbf{n}$ is the unit vector normal to the p-axis. The (p,θ) coordinates represent Radon space. An interesting connection can be drawn between the Radon transform and correlation. If, instead of calculating the angular correlation we calculate the annular correlation. i.e.:

$$R(r) = \int_0^{r_m} \int_0^{2\pi} f(r,\theta)\,\mathrm{rect}\left(\frac{r' + r}{r_o}\right) r'\,dr'\,d\theta \qquad (3)$$

we can obtain a result that is equivalent to the Radon transform averaged over all θ. For simple 2-fold symmetric objects (like a rectangle or ellipse) embedded in backgrounds that can be well-thresholded the result is very nearly the same as a single optimal Radon slice. This result is particularly useful for recovering the re-entrant and multiple-boundary objects mentioned earlier. The combined annular correlation (Radon transform) and angular correlation yield the correct reconstructions for these two cases as shown in Fig's. 4(a) and (b).

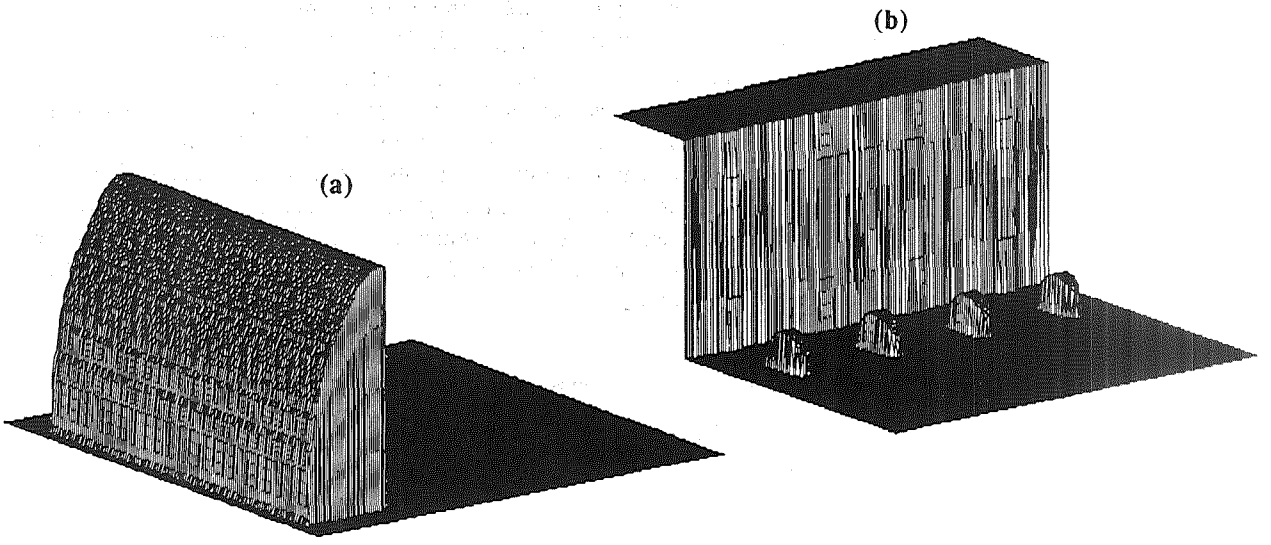

Figure 4. (a) Reconstructed re-entrant boundary shape and (b) multiple boundary shape resulting from the use of angular and annular correlation (or Radon transform).

The Hough transform can also be used to classify objects compared with or without angular correlation, especially 2-fold symmetric objects. If angular correlation is used the angle corresponding to maximum correlation is used to determine the orientation of the object containing the maximum information from the Hough transform. The internal amplitude profile of the object along this orientation is usually the optimal Hough transform slice. Given the orientation and the corresponding profile of an object (or its Fourier components), classification algorithms have been used to identify the object[3]. Primitive features of the object such as length, width, and aspect ratio and orientation derived from angular correlation have also been used along with the Hough transform to improve neural net classification rates[3].

4. SIMULATION OF ANGULAR CORRELATOR

Before implementing the angular correlator optically, it is useful to simulate it on a computer using a set of simple synthetic geometric objects shown in Figure 5. These objects were chosen to include four-fold, three-fold, and two-fold objects as well as an object with multiple boundaries (Figure 5(d)) and an object with a re-entrant boundary (Figure 5(p)). For objects with multiple boundaries, the recovered boundary curve shows the outline of all the objects but not the boundaries between distinct constituent objects. The four-fold objects were chosen to compare shapes with differing image "mass" concentrations (square, plus-sign, rotor, and star) and perturbations from a square (trapezoid, parallelogram, and quadrilateral). The three-fold objects were arranged to compare on the basis of image "mass" concentrations (triangle and three-pointed star) and evidence of bilateral symmetry (isosceles triangle and triangle with concave sides). The two-fold objects were chosen to reflect differences in boundary frequency content (rectangle versus ellipse) and phase (ellipse versus rotated ellipse). For the object with the re-

entrant boundary, the angular correlation algorithm recovers a straight line approximation of the interior concave sides (Figures 3(a) & 5(p)). For the multiple boundary object (five circles), the correlation algorithm does not detect disjoint boundaries (Figures 3(b) & 5(d)). In these two cases, the recovered boundary from the angular correlation algorithm is not sufficient to calculate the exact primitive features of the object or objects within the image. However, as stated before, the Hough transform may be used to recover the internal structure of these objects. Otherwise boundaries of the remaining objects are recovered successfully.

5. OPTICAL HARDWARE

The angular correlator and the Hough transformer can be implemented optically in two basic architectures: time multiplexing (video feedback) or space multiplexing (multiple lenslet arrays). Although the feedback approach was first implemented as described previously[3-4], the preferred implementation is a multi-aperture micro-optical architecture. A multi-aperture optical system to optically rotate an image, calculate its Hough transform and recover its boundary using angular correlation has been conceived[5], and the experimental breadboard is shown in Figure 6. This breadboard includes a video display and collimating lens that serve as the optical interface to represent object space. The actual optical processor is preceded by a zoom lens and (optional) microchannel plate. The microchannel plate forms a real image to be replicated by the multi-lenslet array. It can also be used in a saturated mode to binarize the object. Alternatively the original video display can project through (as a virtual object), or a fiber optic window or binarizing spatial light modulator can be used to create a displayed image. The replicated images are passed through a fixed mask onto a multiple detector array as shown in Fig. 6 (inset(a)). Each detector spatially integrates the superposition of each replicated image and the

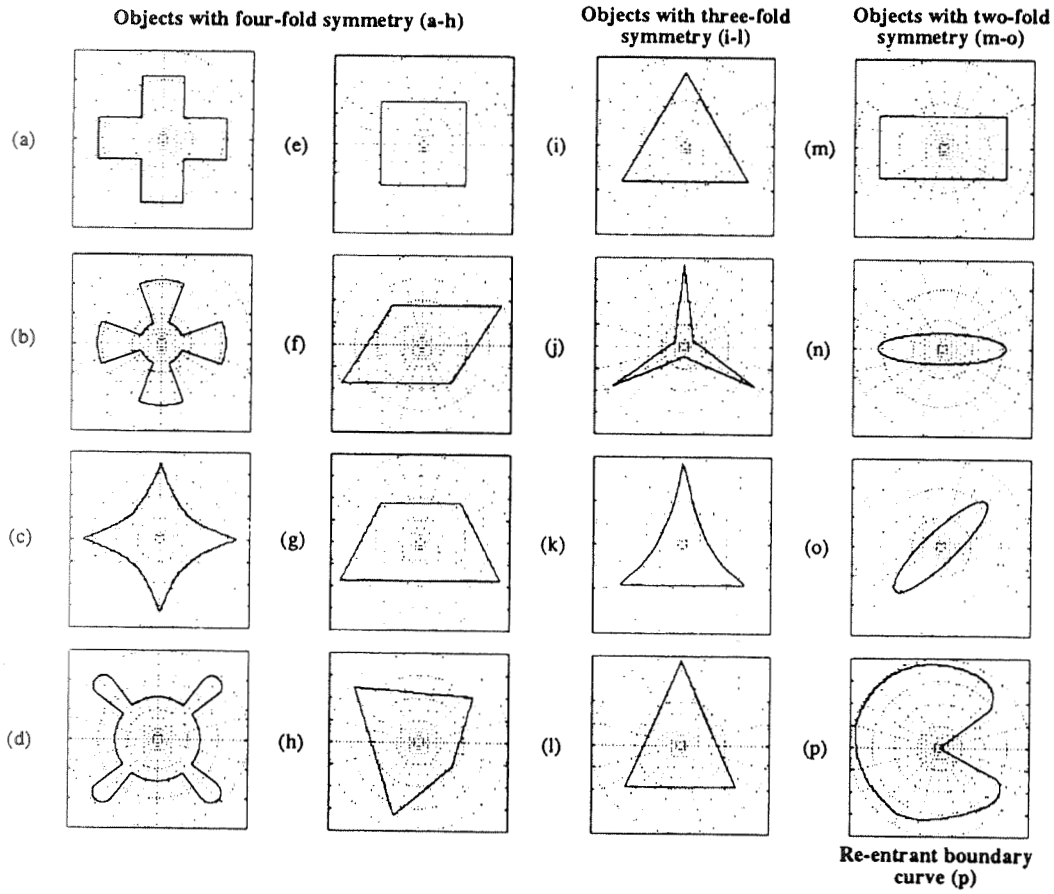

Figure 5. Object boundaries recovered by angular correlation, grouped by symmetry and used to evaluate the neural network simulation.

corresponding mask pattern. For angular correlation the mask consists of a series of rotated half-plane slits as shown in Fig. 6 (inset(b)). For annular correlation (θ-averaged Hough transform) it is a series of annuli as shown in Fig. 6 (inset(c)). Ordinarily, in order to implement the Hough transform, the image has to be rotated. Previous optical architectures use mechanical rotation schemes[6], but mechanical devices have reliability problems and will always be a throughput bottleneck. Replicating the image optically and rotating either the images optically or the pattern elements of the processor mask will substantially increase the throughput and reliability. Other functions can also be performed, such as tracking, using simple mask patterns. The detector outputs are then preamplified, filtered, multiplexed and A/D converted to input into a PC-hosted neural network algorithm discussed in the next section.

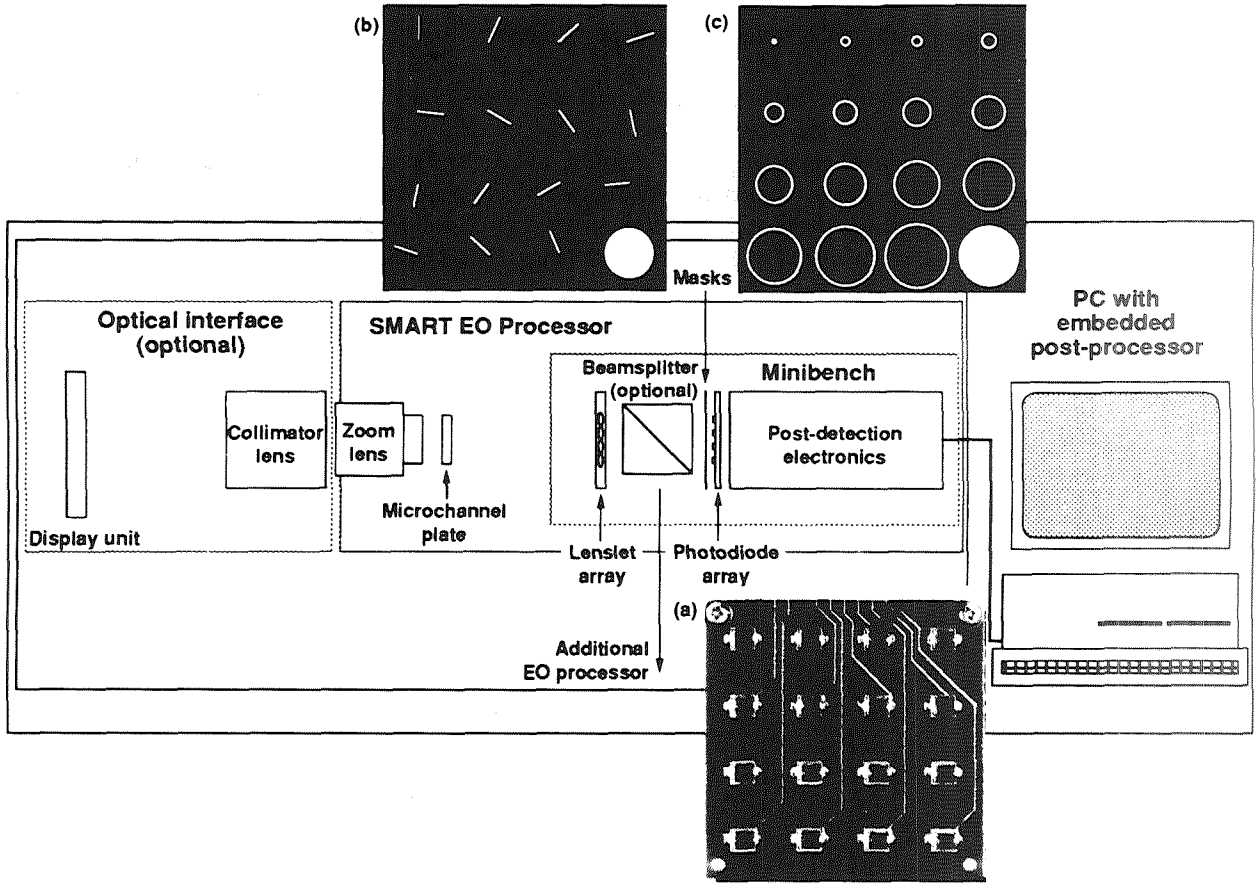

Fig. 6. Optical hardware layout for experimental breadboard optical/digital processor for pattern recognition, showing detector plane (inset a) and masks for angular and annular correlation (insets b and c)

6. DIGITAL NEURAL NETWORK CLASSIFIER EVALUATION

We can easily distinguish between two-fold, three-fold, and four-fold symmetric objects, i.e.: differentiate a rectangle, triangle, and square using symmetry alone. The next higher level of discrimination within the same symmetry class is "bias" or the minimum value of the boundary curve. At this level, image "mass" concentrations (spatially integrated intensities) of objects are compared, as given by the ratio of minimum to maximum radii of the object. The lower the ratio, the greater the image "mass" concentration, (with a minimum of 1 for the circle). For instance, at this level we can separate a rotor from a star. Although it won't be discussed here, Fourier spectra of the boundary can also be used to categorize these objects. This approach is similar to Fourier boundary descriptors described elsewhere[13]

described elsewhere[13]

In this section we will focus on a neural network that uses the boundaries obtained by angular correlation for classification. The angular correlation outputs will be matched against patterns stored in a digital simulation of an analog VLSI neural network under development at APL. This neural network paradigm is a modification of the Bi-directional Associative Memory (BAM) developed by Kosko[14] in which the hidden layer is replaced by a winner-take-all layer[15]. Using the winner-take-all layer eliminates the need for the output to be fed back to the input and eliminates convergence problems prevalent in feedback networks. In the winner-take-all layer, one neuron dominates all other neurons within the layer and allows only one match to occur, thus removing the ambiguity in pattern matching applications. The input patterns are stored as weights of the hidden layer in a bipolar format (off-bits represented by -1 and on-bits represented by +1). The input pattern is fed into the winner-take-all associative memory (WAM), and a binary code representing the matched pattern is the output.

The operation of the WAM can be explained using matrix multiplication. The boundary patterns generated by angular correlation are thresholded, binarized and stored in a pattern matrix. To match the stored patterns against an input pattern, the inner product of the transpose of input vector and the pattern matrix is calculated. An input boundary can then be compared to all of the stored boundaries by forming the correlation matrix. The resulting correlation matrix is a measure of how similar individual stored patterns are to other stored patterns in the pattern matrix. If the correlation matrix has all unity diagonal terms and zero off-diagonal terms, then each input pattern matches itself exactly and is perfectly distinguishable from the other patterns within the pattern matrix. For more details see reference (16).

Figure 5 shows the objects used to test this network. The objects were first presorted according to their symmetry. The re-entrant curve was placed in its own class and was compared with all the objects in the other three symmetry classes. The boundary curves of the presorted objects were binarized with three different threshold levels: median, high and low and stored as rows in separate pattern matrices within each symmetry class. The patterns are also subsampled to 40 data points to simulate more closely the actual VLSI implementation of this network, which stores 116 patterns each 124 bits long. Each of the thresholded versions of each boundary pattern were concatenated, padded with zeros and fed in as a pattern of 124 bits into the WAM simulation. The resulting correlation matrices for the four-fold (**A**), three-fold (**B**), two-fold (**C**) classes, and the re-entrant (**D**) class are:

$$\mathbf{A} = \begin{array}{c} \begin{matrix} \text{(a)} & \text{(b)} & \text{(c)} & \text{(d)} & \text{(e)} & \text{(f)} & \text{(g)} & \text{(h)} \end{matrix} \\ \begin{bmatrix} 1.0000 & 0.5167 & 0.5833 & 0.7333 & 0.7833 & 0.6167 & 0.6167 & 0.5667 \\ 0.5167 & 1.0000 & 0.4667 & 0.3167 & 0.3000 & 0.4333 & 0.4333 & 0.4500 \\ 0.5833 & 0.4667 & 1.0000 & 0.4500 & 0.3667 & 0.9667 & 0.9667 & 0.9833 \\ 0.7333 & 0.3167 & 0.4500 & 1.0000 & 0.9167 & 0.4500 & 0.4500 & 0.4667 \\ 0.7833 & 0.3000 & 0.3667 & 0.9167 & 1.0000 & 0.4000 & 0.4000 & 0.3833 \\ 0.6167 & 0.4333 & 0.9667 & 0.4500 & 0.4000 & 1.0000 & 0.9667 & 0.9500 \\ 0.6167 & 0.4333 & 0.9667 & 0.4500 & 0.4000 & 0.9667 & 1.0000 & 0.9500 \\ 0.5667 & 0.4500 & 0.9833 & 0.4667 & 0.3833 & 0.9500 & 0.9500 & 1.0000 \end{bmatrix} \end{array} \begin{matrix} \text{(a)} \\ \text{(b)} \\ \text{(c)} \\ \text{(d)} \\ \text{(e)} \\ \text{(f)} \\ \text{(g)} \\ \text{(h)} \end{matrix} \tag{4}$$

$$\mathbf{B} = \begin{array}{c} \begin{matrix} \text{(i)} & \text{(j)} & \text{(k)} & \text{(l)} \end{matrix} \\ \begin{bmatrix} 1.0000 & -0.1167 & 0.9000 & 0.4500 \\ -0.1167 & 1.0000 & -0.1167 & 0.3667 \\ 0.9000 & -0.1167 & 1.0000 & 0.3833 \\ 0.4500 & 0.3667 & 0.3833 & 1.0000 \end{bmatrix} \end{array} \begin{matrix} \text{(i)} \\ \text{(j)} \\ \text{(k)} \\ \text{(l)} \end{matrix} \tag{5}$$

$$\mathbf{C} = \begin{array}{c} \begin{matrix} \text{(m)} & \text{(n)} & \text{(o)} \end{matrix} \\ \begin{bmatrix} 1.0000 & 0.3167 & 0.0333 \\ 0.3167 & 1.0000 & 0.0833 \\ 0.0333 & 0.0833 & 1.0000 \end{bmatrix} \end{array} \begin{matrix} \text{(m)} \\ \text{(n)} \\ \text{(o)} \end{matrix} \tag{6}$$

$$\begin{matrix} \text{(a)} & \text{(b)} & \text{(c)} & \text{(d)} & \text{(e)} & \text{(f)} & \text{(g)} & \text{(h)} & \text{(i)} & \text{(j)} & \text{(k)} & \text{(l)} & \text{(m)} & \text{(n)} & \text{(o)} \end{matrix}$$
$$\mathbf{D} = [0.667 \quad 0.214 \quad 0.262 \quad 1 \quad 0.929 \quad 0.262 \quad 0.262 \quad 0.286 \quad 0.357 \quad -0.476 \quad 0.262 \quad 0.190 \quad 0.333 \quad -0.548 \quad -0.190] \tag{7}$$

Under these conditions the patterns are clearly distinguishable from each other. For each column, there is a single maximum value. These results show that if multiple thresholds are used, then boundary curves can be sub-sampled and still be matched using the WAM network. The number of samples needed to adequately sample the boundary function determines the number of channels required for the multi-aperture optical architecture. Since the complexity of the multi-aperture design decreases as the number of channels decrease, sub-sampling the boundary functions and using three thresholds minimizes the number of optical channels needed to compute the angular correlation. Having fewer optical channels also simplifies the interface electronics needed to transfer the detector signals to the neural network. Since the storage capacity of the WAM is limited, as the number of thresholds increases, the amount of boundary samples must decrease. The optimal number of thresholds and the minimum number of samples required is a trade-off issue that is application dependent and requires further study.

7. APPLICATIONS

Some of the applications well suited for this classifier based on angular correlation algorithm include optical parts inspection, machine vision, non-destructive evaluation, medical imaging, strategic surveillance, and tactical missile guidance. For missile guidance, this classifier can be employed in a SAR sensor to recognize targets such as ships. In strategic surveillance the angular correlator can be mated to one of several different sensors which include optical, infrared, SAR, or microwave radiometric sensors. For non-destructive evaluation, the patterns contained in the surface morphology of the test object can be measured using the angular correlator and primitives derived from it. In the area of medical imaging the growth, shape and size of retinal lesions can be measured and tracked over time using this algorithm to recover the boundary of the diseased area. In machine vision, a robot can use this algorithm to recognize, avoid, or manipulate objects using boundaries.

For optical parts inspection, parts traveling down a conveyor belt can be imaged and replicated through the optical interface to extract their boundaries and then sent to the WAM. The WAM matches the part's boundary to one of the stored boundaries. Further action may be taken depending on whether there is a match or not, such as sorting. The parts inspection or sorting task is a well-constrained task. The placement and orientation of the moving parts can be well defined and the boundaries of the parts are well-known. The boundaries can be thresholded to obtain the best match and stored in the pattern matrix. The simplicity of this design makes this correlator compact, reliable and suitable for the factory environment. In this correlator, the throughput is limited by the electronics used to scan the detector array and the WAM. The detector array can be scanned on the order of microseconds and the processing time of the WAM is on the order of 100 microseconds. Thus the correlator should be able to classify objects on a conveyor within 100-200 microseconds, thus making it suitable for fast conveyors.

8. SUMMARY AND CONCLUSION

In this paper we have described angular correlation algorithm that can be used to obtain the boundary of an object. From the boundary, the object can be recognized using a neural network. A winner-take-all associative memory (WAM) network was used to match the object boundaries with stored boundaries. The results from the WAM simulation showed that it is possible to recognize objects based on their boundary. The angular correlation algorithm can be easily implemented using multi-aperture optics to replicate the input object and cross-correlate it with a series of rotated slits. This implementation is well-suited to interface with the WAM for classification. With multiple thresholds, the boundary curves can be decimated and still be recognized by the WAM. Even modified or perturbed objects can be identified using multiple thresholds. The boundary of the object is derived optically in parallel almost instantaneously, and the throughput is limited to less than 100-200 microseconds by the read-out electronics and the WAM classifier. One of the many applications for this hybrid processor is optical parts inspection where a set of objects with known boundaries can be matched to the stored boundaries.

9. ACKNOWLEDGMENT

Discussions with R. E. Jenkins on the neural network simulation and support from J.R. Connelly and W.S. Denny on designing and fabricating detector electronics are gratefully acknowledged.

10. REFERENCES

1. D. Casasent, and D. Psaltis, "New Optical Transforms for Pattern Recognition", Proc. IEEE 65 , 77 (1977)

2. D. Casasent, and D. Psaltis, "Position, rotation and scale invariant optical correlation", Applied Optics 15, 1795 (1976)

3. B. G. Boone, O. B. Shukla, and D. H. Terry, "Extraction of features from images using video feedback", Automatic Object Recognition, Proc. SPIE Vol. 1471, 390 (1991)

4. B. G. Boone, O. B. Shukla, and M. D. Bulla, "Method and Apparatus for Radon Transformation and Angular Correlation in Optical Processors", U. S. patent # 5,101,270, May 7, 1992

5. B. G. Boone, and O. B. Shukla, "SMART Electro-Optical Processor", JHU/APL invention disclosure, Nov. 4, 1991

6. J. P. Crutchfield, "Space-Time Dynamics in Video Feedback", Physics 10D, 229 (1984)

7. J. Cederquist, and S. H. Lee, "The Use of Feedback in Optical Information Processing", Appl. Phys, 18, 311 (1979)

8. G. R. Gindi, and A. F. Gmitro, "Optical feature extraction via the Radon transform", Opt. Eng. 23, 499 (1984)

9. K. Bromley, A. C. H. Louie, R. D. Martin, J. J. Symanski, T. E. Keenan, and M. A. Monahan, "Electro-optical signal processing module", SPIE Vol. 180, Real-Time Signal Processing II, pp. 107-113 (1979)

10. I. Glaser, "Noncoherent optical processor for discrete two-dimensional linear transformations", Optics Letters 5, 449 (1980)

11. M. Agu, A. Akiba, and S. Kamemaru, "Multimatched filtering system as a model of biological visual systems", SPIE Vol. 1014, Micro-Optics, pp. 144-150 (1988)

12. W. A. Christen-Barry, D. H. Terry, and B. G. Boone, "Detection of DNA sequence symmetries using parallel micro-optical devices", SPIE Vol. 1564, Optical Information Processing Systems and Architectures III, pp. 177-188 (1991)

13. E. L. Brill, "Character Recognition via Fourier Descriptors", WESCON, Paper 25/3, Los Angeles, CA (1968)

14. B. Kosko, "Bidirectional associative memories", IEEE Trans. Syst. Man. Cybern., Vol. 18, pp. 49-60, Jan./Feb., 1988

15. K. A. Boahen, P. O. Pouliquen, A. G. Andreou, R. E. Jenkins, "A Heteroassociative Memory Using Current-Mode MOS Analog VLSI Circuits", IEEE Transactions on Circuits and Systems, Vol. 36, No. 5, May, 1989.

16. O.B. Shukla, and B.G. Boone, "Optical Feature Extraction Using the Radon Transform and Angular Correlation", Proc. SPIE Conference on "Optical Information Processing Systems and Architectures IV", Vol. 1771, to be published, presented July 19-24, San Diego, CA